https://doi.org/10.5194/tc-2020-198
Preprint. Discussion started: 12 August 2020

The Cryosphere Discussions

Distributed summer air temperatures across mountain glaciers: climatic sensitivity and glacier size

Thomas E. Shaw[1], Wei Yang[2,3], Álvaro Ayala[4], Claudio Bravo[5], Chuanxi Zhao[2], Francesca Pellicciotti[6,7]

[1] Advanced Mining Technology Center, Universidad de Chile, Santiago, Chile
[2] Key Laboratory of Tibetan Environment Changes and Land Surface Processes, Institute of Tibetan Plateau Research, Chinese Academy of Sciences (CAS), Beijing, China
[3] CAS Center for Excellence in Tibetan Plateau Earth Sciences, Beijing 100101, China
[4] Centre for Advanced Studies in Arid Zones (CEAZA), La Serena, Chile
[5] School of Geography, University of Leeds, Leeds, UK
[6] Federal Institute for Forest, Snow and Landscape Research (WSL), Birmensdorf, Switzerland
[7] Department of Geography, Northumbria University, Newcastle, UK

Corresponding author: Thomas E. Shaw (thomas.shaw@amtc.uchile.cl)

Keywords: Air Temperature, Glaciers, Tibetan Plateau, Climatic Sensitivity

Abstract

Near-surface air temperature (T_a) is highly important for modelling glacier ablation, though its spatio-temporal variability over melting glaciers still remains largely unknown. We present a new dataset of distributed T_a for three glaciers of different size in the south-east Tibetan Plateau during two monsoon-dominated summer seasons. We compare on-glacier T_a to ambient T_a extrapolated from several, local off-glacier stations. We parameterise the along-flowline climatic sensitivity of T_a on these glaciers to changes in off-glacier temperatures and present the results in the context of several available distributed on-glacier datasets around the world. Climatic sensitivity decreases rapidly up to 2000-3000 m along the down-glacier flowline distance. Beyond this distance, both the T_a of the Tibetan glaciers and global glacier datasets show a slower decrease of climatic sensitivity. In general, observations on small glaciers (with < 1000 m flowline distance) are highly sensitive to temperature changes outside the glacier boundary layer. The climatology of a given region can influence the general magnitude of this climatic sensitivity, though no strong relationships are found between along-flowline climatic sensitivity and mean summer temperatures or precipitation. The terminus of some glaciers remain associated with other warm air processes that increase climatic sensitivity (such as divergent boundary layer flow, warm up-valley winds or debris heating effects) which are evident only beyond ~70% of the total glacier flowline distance. Our results therefore suggest a strong role of local effects in modulating climatic sensitivity close to the glacier terminus, although further work is still required to explain the variable presence of these effects for different glaciers.

1. Introduction

Near-surface air temperature (T_a) is one of the dominant controls on glacier energy and mass balance during the ablation season (Petersen et al., 2013; Gabbi et al., 2014; Sauter and Galos, 2016; Maurer et al., 2019; Wang et al., 2019), though modelling its spatio-temporal behaviour above melting ice surfaces remains a challenge. The absence of distributed information regarding T_a has favoured the use of simple, space-time invariant relationships of T_a with elevation, typically

https://doi.org/10.5194/tc-2020-198
Preprint. Discussion started: 12 August 2020

that of the free-air environmental lapse rate (*ELR*). The physical processes of the free-air (that which is independent of the surface boundary layer), however, are not appropriate to describe the variability of T_a for local glacier boundary layers (Figure 1a), especially when the above-ice temperature gradient (within ~10 m of the ice surface) heightens under warm 'ambient' (off-glacier) conditions (van den Broeke, 1997; Greuell and Böhm, 1998; Oerlemans, 2001; Oerlemans and Grisogono, 2002; Ayala et al., 2015). As a result, any extrapolation of T_a observations from an off-glacier location, particularly those at lower elevations, are likely to lead to an overestimation of snow and ice ablation in melt simulations (Petersen and Pellicciotti, 2011; Pellicciotti et al., 2014; Shaw et al., 2017). Whilst this problem has been long understood (Greuell et al., 1997; Greuell and Böhm, 1998), only within the last decade have studies approached it in more detail (Petersen et al., 2013; Ayala et al., 2015; Carturan et al., 2015; Shaw et al., 2017; Bravo et al., 2019; Troxler et al., 2020). Until recently, modelling studies have relied upon simple lapse rates (including the *ELR*) and/or single bias offset values to account for the 'cooling effect' of the near-surface air on-glacier (Arnold et al., 2006; Nolin et al., 2010; Ragettli et al., 2016). The variations of T_a along the glacier flowline (defined following Shea and Moore (2010) as the horizontal distance from an upslope summit or ridge), however, are much more complex (Ayala et al., 2015; Shaw et al., 2017), though a lack of available data usually restricts one's ability to appropriately model this variable. While models applying the degree day approach can make use of off-glacier temperatures as forcing because they are heavily reliant on calibration, for physically based models and models of intermediate complexity (Pellicciotti et al., 2005; Ragettli et al., 2016) it is key to resolve the air temperature distribution over glaciers, especially for turbulent flux calculations.

To date, two main, simplified model approaches have been developed and tested to represent air temperature over glaciers (Figure 1a). The first is the statistical model by Shea and Moore (2010) developed to reconstruct T_a across glaciers of varying size in the Canadian Rockies from ambient temperature records. This approach considered the ratio of observed on-glacier temperature and estimated ambient temperature for the elevation of a given point (hereafter 'T_aAmb') above and below a critical threshold temperature for the onset of the glacier katabatic boundary layer (*KBL*). The parameterisations that operate as a function of the along-flowline distance have since been explored by Carturan et al. (2015) and Shaw et al. (2017) on smaller glaciers in different parts of the Italian Alps. Carturan et al. (2015) found that the original published parameterisations were sufficient to explain T_a on small, fragmenting glaciers up to distances of ~2000m. However, investigation by Shaw et al. (2017) on a small alpine glacier found a pattern of along-flowline T_a that was better described by an alternative, thermodynamic model approach. This second, physically-oriented approach was developed by Ayala et al. (2015) based upon modifications of the original model by Greuell and Böhm (1998) to account for a relative 'warming effect' evident on the termini of some mountain glaciers compared to upper elevations that were fully dominated by katabatic winds. The modified model (termed 'ModGB' in the literature) accounts for the down-glacier cooling of T_a at increasing flowline distances due to sensible heat exchange and adiabatic heating (Greuell and Böhm, 1998). It adds, however, an additional warming factor based upon on-glacier observations in the lower sections of the glacier (e.g. at the greatest flowline distances) to account for additional processes of adiabatic warming (Ayala et al., 2015) (Figure 1a). The ModGB approach has been successively applied at other glacier sites around the world (Shaw et al., 2017; Troxler et al., 2020), though the question of its transferability remains open (Troxler et al., 2020).

Thus the ModGB method operates on the physical principles of the glacier boundary layer (Greuell and Böhm, 1998) though it corrects for relative warming on the lower portion of glacier (Ayala et al., 2015). To establish the magnitude of this warming, however, along-flowline data in the lower portion of the glacier are essential. Because the available distribution of on-glacier observations is often limited and rarely extends for the entire length of the glacier boundary layer, this additional correction for warming and the number of physical unknowns of ModGB can lead to high variability in T_a estimates on the glacier terminus (Troxler et al., 2020) (Figure 1a). In contrast to this, the statistical method of Shea and Moore (2010) provides a more simplified

https://doi.org/10.5194/tc-2020-198
Preprint. Discussion started: 12 August 2020

estimation that has fewer assumptions and parameters, though it does not explicitly account for the physical processes on the glacier, especially those that are thought to be the cause of relative warming for the glacier terminus. It also provides a parameter that more specifically represents the glacier 'climatic sensitivity' of the on-glacier T_a (defined here as the ratio of changes in observed T_a on-glacier to changes in $T_a Amb$). Despite its more conceptual nature, because of its greater generalisability typical of a more simplistic statistical approach, we adopt the Shea and Moore (2010) method to further investigate along-flowline T_a in this study.

To the author's knowledge, no study has investigated the variability of on-glacier T_a at different sites around the world (with the exception of three glaciers considered by Ayala et al., (2015)). As such the transferability or generalisability of models and/or model parameters remain mostly unknown, and analysis of individual glacier sites, while beneficial to process understanding, may not advance the science on how to treat the on-glacier T_a in models. In this study, we make a step toward this by utilising new datasets of on-glacier temperature observations on three glaciers of varying size in the south-east Tibetan Plateau. We analyse the main controls on along-flowline T_a and its climatic sensitivity and present these new findings in the context of 11 other distributed on-glacier observations around the world made to date.
Specifically we aim to i) understand the variability of T_a with the along-flowline distances at three glaciers in the south-east Tibetan Plateau, ii) identify and quantify the climatic sensitivity of on-glacier T_a for different meteorological conditions and glacier sizes and iii) parameterise the along-flowline T_a using the Shea and Moore (2010) method for the Tibetan glaciers and discuss it in the context of globally-derived, published datasets of on-glacier air temperatures.

2. Study Site

The study glaciers are located in the upper Parlung-Zangbo River catchment in the southeast Tibet Plateau (29.24°N, 96.93°E - Figure 2), a region characterised by a summer monsoon climate that typically intrudes via the Brahmaputra Valley (Yang et al., 2011). We present data for three maritime-type valley glaciers in the wider Parlung catchment: Parlung Glacier Number 4 (hereafter 'Parlung4'), Parlung Glacier Number 94 ('Parlung94') and Parlung Glacier Number 390 ('Parlung390'). Parlung4 (Figure 2d) is ~10.8 km^2, north-northeast facing and has an elevation range of 4659-5939 m a.s.l. (Ding et al., 2017). Glaciers Parlung94 (Figure 2c) and Parlung390 (Figure 2e) are smaller valley glaciers (2.51 and 0.37 km^2, respectively) that have termini at higher elevations (elevation ranges of 5000-5635 and 5195-5469 m a.s.l., respectively). The glaciers of the catchment were classified by Yang et al. (2013) as having a spring-accumulation regime and the largest annual rain season of the entire Tibetan Plateau. The upper Parlung River catchment has a mean summer (1979-2019) annual air temperature of ~2°C (at 4600 m a.s.l.), and temperatures in the wider region have been shown to be increasing since the mid 1990's (Yang et al., 2013). The glaciers of this region have been shown to be very sensitive to temperature changes, though with a more elevation-independent mass balance sensitivity compared to other, continental glaciers of the Tibetan Plateau (Wang et al., 2019). The accurate estimation of on-glacier temperatures as Tibetan glaciers shrink and fragment (Carturan et al., 2015) is thus of significant importance for continued modelling efforts. However, to date, no such studies regarding on-glacier temperature distribution have performed within the Tibetan Plateau.

3. Data

3.1. Air temperature observations

We present the observations of T_a from a total of 20 air temperature logger locations (Table 1), 13 of which are situated on-glacier (4680 - 5369 m a.s.l.) and seven off-glacier (4648 - 5168 m a.s.l.). These stations (hereafter referred to as 'T-loggers') observed T_a at a 2 m height using HOBO U23-001 temperature-relative humidity sensors (accuracy +0.21°C) within double-louvered, naturally-ventilated radiation shields mounted on free-standing tripods. The T-loggers recorded data in 10 minute intervals that are averaged to hourly data for analysis. We identify a common observation period over the summers of 2018 and 2019 that range from 12th July – 18th

https://doi.org/10.5194/tc-2020-198
Preprint. Discussion started: 12 August 2020

September. For these date ranges, we observe only small data gaps for some T-loggers (Table 1). We apply the nomenclature of TX_G, whereby X refers to the T-logger number on each glacier and G refers to the glacier number.

We additionally present T_a observations at two automatic weather stations (AWS) at elevations ~4600 m a.s.l. (off-glacier, henceforth 'AWS_Off') and ~4650 m a.s.l. (on Parlung4, henceforth 'AWS_On') for the same time period (Figure 2). For distributing off-glacier air temperature, we consider AWS_Off as our reference station. The AWS T_a observations are provided by Vaisala HMP60 temperature-relative humidity sensors (accuracy +0.5°C) also housed in naturally-ventilated radiation shields.

3.2. *Uncertainty of air temperature observations*

To provide an estimate of observation uncertainty, we compared the hourly divergence of two naturally-ventilated T_a observations for the whole period between $T4_4$ and AWS_On (Figure 2d), that are co-located within a few metres of horizontal distance on Parlung4 Glacier. A test of absolute differences between the two stations resulted in a mean of < 0.4°C for all hours (n = 3312) and ~0.5°C for the warmest 10% of the hours of ambient temperature at AWS_Off (hereafter referred to as 'P90' - (Ayala et al., 2015; Shaw et al., 2017; Troxler et al., 2020)). We find that for these hours (when the *KBL* development is theoretically at its strongest (e.g. van den Broeke, 1997; Oerlemans and Grisogono, 2002)), that 95% of hourly differences were < 1°C (Figure S1). For on-glacier stations at large flowline distances (Figure 2), these large uncertainties are considered less likely given the good ventilation provided to the sensors within the *KBL*. While observations at short flowline distances with calm conditions and high incoming radiation may result in maximum uncertainties up to ~1°C (Troxler et al., 2020), we apply a ±0.5°C uncertainty for analysis of distributed T_a. For the instantaneous differences > 1°C, wind speeds at AWS_On were <2 m s^{-1}. Wind speeds for P90 conditions were otherwise in excess of 3-4 m s^{-1}, though no other observations of on-glacier wind speed are available at higher elevations.

3.3. *Meteorological information*

We obtained information regarding T_a, incoming shortwave radiation and relative humidity (AWS_Off), on-glacier wind speed (AWS_On) and 'free-air' wind speed and direction (ERA5 - C3S, 2017). We used these data to explore the relationships of hourly on- and off-glacier temperatures (section 4.2) for different prevailing conditions.

3.4. *Elevation information*

We used the 12.5 m Alos Palsar (ASF DAAC, 2020) digital elevation model (DEM) to provide elevation information for the catchment (Figure 2b). We utilised this DEM in order to calculate flowline distances (m) for each glacier from the TopoToolbox functions in Matlab (Schwanghart and Kuhn, 2010), following Troxler et al, (2020). We note that the methodology for flowline generation is not currently uniform among all studies of this type (Shea and Moore, 2010; Ayala et al., 2015; Carturan et al., 2015; Shaw et al., 2017; Bravo et al., 2019; Troxler et al., 2020) and may produce some differences in the calculated distances close to the lateral borders of the glaciers. In addition, the generated flowlines may also be dependent upon the quality and resolution of the DEM available between the aforementioned studies. However, we do not analyse lateral T_a variations in this study and consider that the impact of varying methods for flowline generation to be negligible when assessing observations at a few select points on the glacier.

4. Methods

For this study we use local, off-glacier T_a data from AWS_Off for aggregation of on-glacier sub-groups or for distribution of T_a in space. Sub-grouping allows one to interpret general causal

https://doi.org/10.5194/tc-2020-198
Preprint. Discussion started: 12 August 2020

factors that dictate on-glacier behaviour, whereas the distribution in space allows a direct comparison of on- and off-glacier temperatures and the effect of the glacier boundary layer. The following subsections outline the sub-grouping (4.1) and distribution (4.2) methodologies. The model parameterisations of Shea and Moore (2010) and application to Tibetan and global datasets are considered in sections 4.3 and 4.4, respectively.

4.1. Sub-grouping on-glacier air temperature observations

We sub-group our on-glacier observations by 10th and 90th percentiles (P10/P90) of off-glacier T_a at AWS_Off (Figure 2a) that have been shown to relate to the development of the glacier boundary layer (Ayala et al., 2015). Following the methodology of previous studies (Ayala et al., 2015; Shaw et al., 2017; Troxler et al., 2020), we consider all contemporaneous observations of on-glacier T_a at each T-logger that relate to the same hours as the P10/P90 classification at AWS_Off. We consider the deviation from a linear relationship of T_a with elevation and flowline distance for these subgroups, assessing this 'linearity' by use of the coefficient of determination (R^2). For a comparison to previous studies (Petersen and Pellicciotti, 2011; Shaw et al., 2017), we also report the equivalent on-glacier lapse rate that would be calculated for the above conditions.

4.2. Comparison of on- and off-glacier air temperature

We extrapolate AWS_Off T_a records to the elevation of each on-glacier T-logger (Table 1) to quantify the T_a differences within the glacier boundary layer (Figure 1a). We derive an hourly variable lapse rate between AWS_Off and off-glacier T-loggers deemed to be independent of the glacier wind layer, thus excluding those T-loggers in the immediate pro-glacial zones. Specifically, we use AWS_Off and T-loggers $T1_{94}$, $T2_{94}$ and $T1_{390}$ to construct a 'catchment lapse rate' where the origin of the calculated regression must pass through the elevation of AWS_Off that acts as the forcing station in this study (see supplementary information, Figure S2). We consider this as the best available approach to estimate the ambient lapse rate for the catchment. We compare the hourly estimates of extrapolated off-glacier T_a (*T_aAmb)* with the observations at each on-glacier T-logger in order to i) understand how large the T_a offset (bias) is at each site and how it relates to meteorological conditions and glacier flowline distance; and ii) parameterise the along flowline climatic sensitivity to *T_aAmb* following Shea and Moore (2010) (section 4.3).

4.3. Estimation of on-glacier climatic sensitivity

The Shea and Moore (2010) approach (hereafter 'SM10') estimates on-glacier T_a using *T_aAmb* at a given elevation by:

$$Ta = \begin{cases} T1 + k2(T_aAmb - T*), & T_aAmb \geq T* \\ T1 - k1(T* - T_aAmb), & T_aAmb < T* \end{cases} \tag{1}$$

where *T** (°C) represents the threshold ambient temperature for the onset of katabatic flow and *T1* is the corresponding threshold T_a on the glacier. Parameters *k1* and *k2* are the climatic sensitivities of on-glacier T_a to *T_aAmb* below and above the threshold *T** (Figure 1b and c). *k1* and *k2* were parameterised in the original study using exponential functions of the along flowline distance (*DF*):

$$k1 = \beta 1 \exp(\beta 2\, DF) \tag{2}$$

$$k2 = \beta 3 + \beta 4 \exp(\beta 5\, DF) \tag{3}$$

https://doi.org/10.5194/tc-2020-198
Preprint. Discussion started: 12 August 2020

where βi are the fitted coefficients. Following the suggestion of Carturan et al. (2015), we implement a relation against the flowline that estimates the threshold temperature for onset of katabatic effects (T^*) at a given distance as:

$$T* = \frac{C1DF}{C2 + DF} \tag{4}$$

where *C1* (6.61) and *C2* (436.04) are the fitted coefficients of Carturan et al. (2015). We calculate *k1* and *k2* at each T-logger station using the linear regression of observed T_a and T_aAmb above and below T^* (Figure 1) as derived from equation 4. We note that the parameter *k2* holds a greater significance for modelling T_a (Figure 1a), as this more closely represents the climatic sensitivity reported by previous works (Greuell et al., 1997; Greuell and Böhm, 1998; Oerlemans, 2001; 2010), whereas *k1* represents the ratio of above-glacier and free-air temperatures without a katabatic effect that have been shown to relate more closely to T_aAmb (Shea and Moore, 2010; Shaw et al., 2017). For this study, we therefore pay particular attention to the *k2* sensitivities on the Parlung glaciers and assess their relationship to along-flowline distance.

4.3. *Global datasets of on-glacier temperatures*

To explore the generalisability of the SM10 approach and provide context to the findings of the Parlung catchment, we explore the calculated *k1* and *k2* parameters for several of the available distributed on-glacier datasets published to date (Figure S3, Table 2). We subset summer periods to when all available on-glacier observations are available at a given site. For sites of the Coastal Mountains of British Columbia ('CMBC' - Shea and Moore, 2010) and Alta Val de La Mare ('AVDM' - Carturan et al., 2015), we apply the published parameter sets derived from those authors. For all other sites, we derive T_aAmb from the most locally available off-glacier AWS and the published lapse rate from the relevant studies (Table 2). In the absence of lapse rate information, we apply the *ELR* (-6.5°C km^{-1}) to extrapolate T_a to the elevation of the on-glacier observations.

For each glacier site, data are limited to those hours when all stations for that glacier are available and the *k1* and *k2* parameters (equation 1) are only calculated when; i), >10% of the total hourly data at a given station is above or below T^* (to have enough data to calculate *k2* and *k1*, respectively) and, ii) the linear regression to derive each parameter is significant to the 0.95 level. For those on-glacier stations that do not satisfy the above requirements, we do not calculate the *k1* and *k2* parameters.

Finally, we group the derived *k2* sensitivities of the SM10 approach against the climatology that describes the given glacier(s) location. For this, we consider the mean summer (JJAS or DJFM in the southern hemisphere) air temperature (MSAT) and the total annual precipitation for the year(s) of study at each location (Table 2). MSAT is derived from the ERA5 product for the glacier centroid location and corrected to the mean glacier elevation by the *ELR*. However, total precipitation from ERA5 has been shown to have considerable bias when tested against in-situ observations (e.g. Betts et al., 2019), and so we provide the best available value from the relevant literature (Table 2). We note that a full analysis of the local climate is beyond the scope of this work, though we attempted a generalised analysis in order to link any clear differences in the global datasets to climatological influences.

5. Results

5.1. *Variability of on-glacier air temperatures*

Figure 3 shows the mean T_a as a function of elevation and flowline distance for the Parlung glaciers for all conditions and for the warmest 10% of AWS_Off observations (P90). The average of all hours reveals a generally linear relationship with the glacier elevation (Figure 3a) and flowline (Figure 3b), resulting in mean on-glacier lapse rate (mean R^2 with elevation) equivalent to -3.0°C km^{-1} (0.92), -3.7°C km^{-1} (0.71) and -4.5°C km^{-1} (0.81) for Parlung4, Parlung94 and Parlung390, respectively. For P90 hours (n = 312), mean T_a demonstrates a poorer fit to elevation and flowline for Parlung4 (mean R^2 with elevation = 0.12, and flowline = 0.20) and Parlung 94 (mean R^2 with elevation = 0.13 and flowline = 0.09). For the small Parlung390 Glacier, T_a remains strongly related to elevation (R^2 = 0.84) and flowline (R^2 = 0.82) under P90 conditions. The equivalent mean on-glacier 'lapse rates' for P90 hours are -2.1°C km^{-1}, -1.4°C km^{-1} and -4.1°C km^{-1}. Nevertheless, assuming a calculated 0.5°C uncertainty of the observations for P90 conditions (Figure 3c and d), the mean of observations still lies along a linear fit line. However, for given hours, the deviation of observations from the linear fit line exceeds 3°C at large flowline distances (> 7000 m) on Parlung4. In general, 2018 experienced cooler average temperatures at higher elevations, but in general, there are no marked differences between the two years of observation when comparing to glacier elevation or flowline (not shown).

5.2. Differences in on- and off-glacier air temperatures

Comparing mean on- and off-glacier T_a reveals the expected behaviour associated with the glacier 'cooling effect' (Carturan et al., 2015) and a greater deviation from the calculated catchment lapse rate for the warmest conditions (P90, Figure 4), indicating a reduced climatic sensitivity. The mean T_a observed at off-glacier T-Loggers supports the selection of those stations used for catchment lapse rate calculation (green dots in Figure 4) that are further from the potential effects of the glacier boundary layer (red markers in Figure 4). Following Carturan et al. (2015), we suggest a potential non-linear behaviour of lapse rates between AWS_Off and the top of the flowline for Parlung390, though we lack the off-glacier observations above the flowline origin to test this (Figure 4b). We therefore utilise a piecewise lapse rate at the point of the highest off-glacier lapse rate station ($T1_{390}$ - red line in Figure 4) to account for the discrepancy between the estimated and observed T_a at $T6_{390}$, which is assumed to be near to the flowline origin where climatic sensitivity is theoretically equal to 1 (i.e. that on-glacier observations = $T_a amb$).

Figure 5 presents the hourly differences between T_aAmb and observed T_a at each site. The deviation of estimated and observed T_a theoretically begins at a critical temperature threshold, T^* (Shea and Moore, 2010) and this effect can be observed at T-logger sites on Parlung94 and Parlung4, particularly those at greater flowline distances. Coloured by the hourly wind speeds recorded at AWS_On, the beginning of the temperature deviations (T^*) aligns well with the onset of katabatic winds on Parlung4 (and only assumed for the other glaciers due to lack of on-glacier wind observations – Figure 5). Despite being pro-glacial stations, $T1_4$ and $T2_4$ reveal a similar, albeit weaker effect of the glacier boundary layer, possibly due to larger glacier flowline and sustained effect of the katabatic wind into the pro-glacial area.

The mean bias offset of along-flowline T_a using the catchment lapse rate is shown in Figure 6. For the coolest 10% of hours at AWS_Off (P10), there is generally minimal offset between T_aAmb and observed T_a for the entire dataset. This clearly does not hold true for P90 conditions (Figure 6a), as already established (Figure 4), and offsets of T_a (T_aAmb – observed T_a) are up to 5.8°C at flowline distances of > 7000 m on Parlung4. These effects appear to heighten beyond 2000 m along the flowline (Parlung94), though slight offsets can be witnessed for all glaciers. This is generally associated with drier conditions, and for hours of greater relative humidity (AWS_Off), offsets are small (Figure 6b). Considering 'free-air' wind variability provided by ERA5 reanalysis, T_a offsets are largest for the dominant south-westerly wind direction (85% of hours) and when free-air wind speeds are smallest (Figure 6c and 6d). However, un-corrected, gridded wind speeds do not appropriately represent the local 'free-air' boundary conditions and thus the interaction of off-glacier wind speeds and the glacier boundary layer development remain unclear for these glaciers. For all but the coolest ambient temperatures (Figure 6a), observations at the greatest flowline distances deviate the most from the estimated values.

This offset is highly variable in time, however, and related to the prevailing conditions of a given year (Figure 7). Considering the maximum daily T_a offsets at the on-glacier T-Logger closest to the terminus on each glacier (Table 1), we find that Parlung94 and Parlung4 T-loggers have similar magnitudes of T_a offsets during the mid-summer months, particularly for 2018 (Figure 7). These maximum offsets are in clear relation to the incoming shortwave radiation record at AWS_Off (correlations of 0.44, 0.60 and 0.80 for Parlung390, Parlung94 and Parlung4, respectively), which are indicative of warmer ambient conditions (i.e. P90). For Parlung390 this offset is much smaller, though varies considerably throughout the summer. For 2019, maximum daily T_a offsets on Parlung390 steadily increase during July and August then fall close to zero in September. The bias offsets for Parlung4 and Parlung94, however, remain sizeable (Figure 7). Because our study period focuses on the core monsoon period (Yang et al., 2011), we do not observe the influence of monsoon arrival or cessation on the T_a variability of the Parlung Glaciers.

5.3. Parameterisation of along-flowline air temperatures

Figure 8 presents the SM10 parameterisations for the Parlung glaciers in comparison to those derived for the available distributed T_a datasets around the world (Table 2). Comparing the *k1* and *k2* parameters from Tibet to the original parameters of Shea and Moore (2010), a similar behaviour is observable for both sites up to ~2000-3000 m of flowline distance (red and blue dashed lines), though there exists a larger variability in the calculated parameters at longer flowline distances on Parlung4 (Figure 8). Accordingly, the exponential functions that are fitted to the observations at Parlung glaciers and the original study are notably distinct (Figure 8, Table 3). This behaviour is further highlighted when observing other published or revised datasets for the context of this work (Figure 8b). A 'global' parameterisation for all sites where down-glacier decrease in climatic sensitivity is evident (black dashed lines in Figure 8) clearly misrepresents many of the observations, particularly those at greater flowline distances, balancing the behaviours reported for different sites.
Notably, observations at McCall Glacier, Alaska relate very well to ambient T_a under cooler conditions, with all *k1* values remaining > 0.9. Above the T^* threshold, however, the relationship of observed and estimated T_a results in increasing *k2* along the flowline, in contradiction to the majority of the other datasets. Nevertheless, this data also confirms the increased climatic sensitivity on the glacier terminus (Troxler et al., 2020) as evident with datasets for Tsanteleina (Shaw et al., 2017), Arolla and Juncal Norte (Ayala et al., 2015). Observations at Parlung4 and Universidad Glacier (Bravo et al., 2017) emphasise the strong decrease in climatic sensitivity at large flowline distances (~10,000 m) previously only witnessed from one location on Bridge Glacier, Canada (Shea and Moore, 2010).

Figure 9 shows the *k2* parameters plotted against flowline distance, coloured by rankings of MSAT and precipitation totals (Table 2). The warmest of the investigation sites (during the measurement years) appear to lie closer along the original SM10 parameterisation until ~4000 m, whereas deviation of the *k2* parameters from this line appears larger for observations at relatively cold sites (Greve, McCall and Arolla – Figure 9a). The main exception to this is for Juncal Norte (Petersen and Pellicciotti, 2011; Ayala et al., 2015), which demonstrates a high and rapidly increasing sensitivity of ambient T_a at the greatest flowline distances.
No clear patterns are visible with relation to mean annual precipitation totals, although the observations at Juncal Norte are noted as the driest of the study sites (Figure 9b).
A clear difference between observations of CMBC and Parlung at large flowline distances is the distance from the glacier terminus, which suggests a possible difference in processes being compared between sites. Accordingly, we plot the *k2* parameters as a function of the normalised flowline, adjusted by the total length of glacier under the year(s) of observation (Table 2). A slight trend toward lower *k2* values (lower sensitivity to ambient T_a) is observable for relatively warmer regions, though no clear pattern emerges for MSAT (Figure 9c) or precipitation totals (Figure 9d). The largest flowline distance observation of the entire dataset (Figure 9a) in fact extends only ~60% of the total glacier length (Bridge Glacier - CMBC), neither representing the smallest climatic sensitivity (Figure 8b), nor the increasing climatic sensitivity witnessed at the terminus of the glacier by other studies (Ayala et al., 2015). In fact, by subjectively grouping glacier sites

https://doi.org/10.5194/tc-2020-198
Preprint. Discussion started: 12 August 2020

by the presence of the relative down-glacier cooling (decreasing sensitivity) and warming (decreasing followed by increasing sensitivity) along the total glacier length, one can observe that this effect is absent for the both smaller and larger glaciers (Figure 10a), albeit limited by lack of observations across an entire glacier in most cases. For those glaciers where the pattern of down-glacier sensitivity increase ('relative warming effect') is evident, it is found only beyond ~70% of the total glacier flowline distance (Figure 10b – vertical dashed line). Up to this distance, no increase in *k2* sensitivity is seen from the data.

6. Discussion

6.1. Relevance of the findings from Parlung Glaciers

The observations of along-flowline T_a on the glaciers in the Parlung catchment add yet more evidence of the spatial variability of the glacier cooling and dampening effect (Oerlemans, 2001; Carturan et al., 2015; Shaw et al., 2017) and the need to appropriately estimate its behaviour for use in glacier melt models (Petersen and Pellicciotti, 2011; Shaw et al., 2017; Bravo et al., 2019). It has long since been observed that a static lapse rate is inappropriate for characterising the spatio-temporal variability of T_a, both within the *KBL* (Greuell et al., 1997; Konya et al., 2007; Marshall et al., 2007; Gardner et al., 2009; Petersen and Pellicciotti, 2011) and outside the glacier boundary layer in adjacent valleys (Minder et al., 2010; Immerzeel et al., 2014; Gabbi et al., 2014; Heynen et al., 2016; Jobst et al., 2016). Despite this, the lack of locally available observations often requires modellers to force model simulations with the nearest off-glacier record of T_a and extrapolate it based upon the *ELR* value as a default. In the case of Tibetan glaciers, model studies have often derived static lapse rates between on-and off-glacier stations (Huintjes et al., 2015) or used static values to extrapolate or downscale T_a with a correction based upon a single on-glacier location (e.g. Caidong and Sorteberg, 2010; Yang et al., 2013; Zhao et al., 2014). To the author's knowledge, this is the first time that such detailed information regarding spatio-temporal variations in T_a have been presented for a glacier of the Tibetan Plateau. Because glaciers of the south-eastern Tibetan Plateau have been shown to be particularly susceptible to increases in T_a (Wang et al., 2019), accurately parameterising T_a along glaciers of differing size is highly relevant for present and future melt modelling attempts. This is especially true where glaciers begin to shrink or fragment (Munro and Marosz-Wantuch, 2009; Jiskoot and Mueller, 2012; Carturan et al., 2015) and become more sensitive to ambient air temperatures due to a lack of katabatic boundary layer development (Figures 6 and 7).

The summer monsoon exerts a strong control on the energy and mass balance of Tibetan glaciers (Yang et al., 2011; Mölg et al., 2012; Zhu et al., 2015). Although our dataset spanned two summers of only the core monsoon period for this region (Yang et al., 2011), we have shown that the sensitivity of the glacier to external temperature changes (shown by T_a bias offsets) has a sizeable temporal variability that can be controlled by the monsoon weather conditions (such as ambient air temperature, humidity and incoming radiation) and can sometimes be independent of the glacier size (Figure 7). Whilst we cannot determine the impact of monsoon timing and intensity upon the climatic sensitivity of these glaciers with the current dataset, we are able to determine that the observed relationship to flowline distance is consistent to that of other regions of the world (Figure 8). Future work on Tibetan glaciers should attempt to extend monitoring to the pre-monsoon period to identify if a seasonal onset for the changing glacier climatic sensitivity can be defined, and how the monsoon may affect it. Particular focus should be given to understand the local meteorological conditions for each glacier, as this may explain some of the variability in T_a offset values, and why they may sometimes be independent of the along-flowline distance (Figure 7).

6.2. Parameterising glacier climatic sensitivity

In this study, we discuss the climatic sensitivity of on-glacier T_a based upon observations above a threshold ambient temperature for the onset of katabatic conditions (T^*). This sensitivity to ambient temperature during relatively warm conditions, indicated by the *k2* parameter of Shea and Moore (2010)(Figure 1), demonstrates a generally consistent behaviour between the T-logger observations of Parlung glaciers and those where this model had been previously implemented (Shea and Moore, 2010; Carturan et al., 2015). It also resulted in a similar parameterisation, albeit with a slightly greater sensitivity to the ambient temperature (i.e. larger *k2* values - Figure 8b). Whilst the newly presented dataset for the Parlung catchment provides an important confirmation of the climatic sensitivity for some Tibetan glaciers, further studies of individual glaciers can provide only local parameterisations for climatic sensitivity that may not be applicable to other sites. Accordingly, we have made here a first attempt at combining many of the published datasets regarding distributed T_a on mountain glaciers around the world (Table 2) to examine the potential for generalisability of a model accounting for climatic sensitivity (Figure 8).

We found a sizeable spread in the climatic sensitivities of T_a for the on-glacier datasets considered, though a consistently rapid decrease of sensitivity along glacier flowlines is found for most sites up until ~2000-3000 m of distance (Figure 8b). While localised meteorological and topographic factors likely interact to explain the spread of sensitivities at small flowline distances (Figure 8b), the results suggest that small glaciers with flow lengths < 1000 m would reflect a 0.7-0.8 sensitivity to changes in T_aAmb. Beyond this distance, the climatic sensitivities notably follow one of two patterns; a continued, albeit less rapid decrease in sensitivity (more generally following the model proposed by Shea and Moore (2010)), or a tendency toward increasing sensitivity at the largest flowline distances (more related to those findings of the 'ModGB' model - Figure 1a). With reference to the relative T_a differences among only on-glacier observations, these have been termed as down-glacier 'cooling' or 'warming', respectively for many past studies (Ayala et al., 2015; Carturan et al., 2015; Shaw et al., 2017; Troxler et al., 2020). Whilst the former is generally associated with relatively warmer regions of study (Figure 9), such as the Canadian Rockies (Shea and Moore, 2010) or Universidad Glacier (Bravo et al., 2017), no strong relationship of the climate setting exists between these sites to explain the magnitude of the climatic sensitivity (i.e. the strength of the glacier cooling and dampening effect) nor the observed increases in climatic sensitivity on glacier termini (Ayala et al., 2015; Shaw et al., 2017; Troxler et al., 2020).

Interestingly, we noted that the most distant station observation used to derive the parameterisation by Shea and Moore (2010) was located only around 60% of the total glacier flowline distance (Bridge Glacier - Figure 10), whereas data presented by other studies, provided observations up to the glacier terminus (Greuell and Böhm, 1998; Ayala et al., 2015; Shaw et al., 2017; Troxler et al., 2020), therefore potentially parameterising different effects of the glacier boundary layer. It has been suggested that observations at large flowline distances (such as that on Parlung4 or Bridge Glacier) represent a segment of the boundary layer where the near-surface layer becomes highly insensitive to the ambient free-air temperature fluctuations (point '3' in Figure 1a and d). This phenomenon has been shown to be sustained over large fetch distances by an increasing depth of the glacier wind layer (van den Broeke et al., 1997; Greuell and Böhm, 1998; Shea and Moore, 2010, Jiskoot and Mueller, 2012). However, as air parcels travel down-glacier toward the glacier terminus (point '4' in Figure 1a and d), they potentially encounter warm air entrainment due to a divergent boundary layer (Munro, 2006), up-valley winds (Pellicciotti et al., 2008; Oerlemans, 2010; Petersen and Pellicciotti, 2011) or heating from debris-covered ice at the terminus (Brock et al., 2010; Shaw et al., 2016; Steiner and Pellicciotti, 2016; Bonekamp et al., 2020). These are effects of the glacier boundary layer that the ModGB model was designed to account for, though we did not explicitly test this within our study due to a requirement for more data and a greater number of parameters and assumptions (Shaw et al., 2017). The strength of this so called along-glacier 'warming effect' could therefore be governed by local topography (adjusting the boundary layer convergence or divergence) or the total glacier flowline distance and the large fetch of a cool air parcel overcoming the competing effect of warm, up-valley winds (Figure 1d - as seen at $T2_4$ in Figure 5).

By subjectively grouping glaciers by the presence of the observed increase in climatic sensitivity and normalising the flowline distance of the observations by the total flowline for each glacier, we identify that the relative increases in climatic sensitivity begin at ~ 70% of the total flowline distance (Figure 10). A smaller climatic sensitivity can be observed for larger glaciers (Figure

https://doi.org/10.5194/tc-2020-198
Preprint. Discussion started: 12 August 2020

10a), which is consistent with the development of the *KBL* over a large fetch (Greuell and Böhm, 1998; Shea and Moore, 2010), though the length itself indicates nothing clear about why greater climatic sensitivity exists for some glacier termini (Figure 10b).

The clear outlier of these datasets is Juncal Norte Glacier in Chile (Figure 8b). It is interesting to note that Juncal Norte is the only reported case in the literature on T_a variability where the warmest hours of the afternoon correspond to the dominance of an up-valley, off-glacier wind (Pellicciotti et al., 2008; Petersen and Pellicciotti, 2011). Counter to the typical role of the dominant, down-glacier wind layer for these warmest afternoon hours (Greuell et al., 1997; Greuell and Böhm, 1998; Strasser et al., 2004; Jiskoot and Mueller, 2012; Shaw et al., 2017; Troxler et al., 2020), up-valley winds on Juncal Norte seemingly erode the along-flowline reduction in climatic sensitivity (along-flowline cooling) up to a distance along the flowline where it is theoretically at its maximum (point ‘3’ in Figure 1). Evidence from other glaciers suggest that this point is close to upper observations for Juncal Norte at ~70% of the total flowline (Figure 10b), though further observations would be required to test this.

6.3. Future directions for researching air temperatures on glaciers

A limitation of our work is the dependency of the derived ‘global’ climatic sensitivities (Figure 8b) to the available off-glacier data and the published lapse rates to extrapolate them to the relevant elevations on-glacier. In our case, we are able to identify a potentially non-linear lapse rate of T_a*Amb* for the highest elevations over Parlung94 and Parlung390 (Figure 4). Although we cannot confirm this without off-glacier observations above the top of the flowline (Carturan et al., 2015), we are able to well constrain ambient air temperature distribution using hourly observations at several off-glacier locations to derive the best possible ‘catchment lapse rate’. For other datasets (Table 2), we rely upon the available off-glacier data and lapse rates that are not derived in a consistent manner. The derivation of flowline distances from the DEM are also not consistent between the prior studies (Shea and Moore, 2010; Carturan et al., 2015; Shaw et al., 2017; Bravo et al., 2019; Troxler et al., 2020), and may hold some small influence on the derived parameterisations (Table 3), particularly at lateral locations on the glacier (not explored here), that can be subject to different micro-meteorological effects (van de Wal, 1992; Hannah et al., 2000; Shaw et al., 2017). Equally, the uncertainty of the actual observations (e.g. section 3.2) is hard to clearly define due the variable instrumentation (sensors and radiation shielding), on-glacier location and local topographic and micro-meteorological effects of each study site (Table 2). Further work on a unified model of estimating T_a should need to address these issues, perhaps with further, dedicated analyses.

In our study, we apply the parameterisation of Carturan et al. (2015) to derive along-flowline values of the theoretical onset of the *KBL* (T^*). While these values appear appropriate for our case studies (based upon manual inspection), they were derived for a more limited number of total observations. We experimented with a static T^* value of 5°C in order to test the sensitivity of our analysis to the assumptions of T^*, though found a minimal change in our derived *k2* sensitivities (not shown).

Finally, in this study we assess climatic sensitivity based upon ambient air temperatures above this T^* threshold. We identify, however, that this is partly different to the climatic sensitivity presented by earlier works (Greuell et al., 1997; Greuell and Böhm, 1998; Oerlemans, 2001; 2010), which considered all hours of the on-glacier observations when comparing to extrapolated off-glacier T_a. In some instances, over estimation of on-glacier T_a also for cooler conditions may produce a consistent ‘all-hour’ climatic sensitivity value (i.e. where *k1* and *k2* sensitivities are similar - Figure 1b). However, ignoring separate effects (*k1* and *k2*) due the rise of the *KBL* (Figure 1c, Figure 5) arguably over-simplifies the glacier’s climatic sensitivity and therefore does not aptly describe the two behaviours separated by an onset event (Shea and Moore, 2010; Jiskoot and Mueller, 2012). Accordingly, we caution somewhat the direct comparison of the climatic sensitivity presented here and that of previous works, though consider the use of *k2* to be an appropriate indicator of climatic sensitivity for this work going forward. As previously

https://doi.org/10.5194/tc-2020-198
Preprint. Discussion started: 12 August 2020

mentioned, we have considered the approach of Shea and Moore (2010) to be a more generalizable method for calculating glacier climatic sensitivity and thus estimating on-glacier T_a. However, the competing effects of glacier katabatic and up-valley winds need to be incorporated to address the challenges that less simplistic methods (i.e. ModGB) were designed for.

Based upon the findings of this work, we recommend that future research i) attempt to standardise, where possible, the measurement and comparison of off- and on-glacier air temperature, potentially exploring more the use of artificially-ventilated radiation shields that are less prone to heating errors (Georges and Kaser, 2002), ii) instrument glaciers of varying size in the same catchment to explore the relative importance of glacier size and local meteorological conditions (Figure 7), and iii) model the detailed interactions of air flows on the glacier termini using, for example, large eddy simulations (Sauter and Galos, 2016; Bonekamp et al., 2020) in order to identify possible drivers of the observed increase in climatic sensitivity for certain glaciers (point '4' in Figure 1).

7. Conclusions

We presented a new dataset of distributed on-glacier air temperatures for three glaciers of different size in the south-east Tibetan Plateau during two summers (July - September). We analysed the along-flowline air temperature distribution for all three glaciers and compared them to the estimated ambient temperatures derived from several, local off-glacier stations. Using this information, we parameterised the along-flowline climatic sensitivities of these glaciers using the method proposed by Shea and Moore (2010) and presented the results in the context of several available distributed on-glacier datasets to date. The key findings of this work are:

1. For our Tibetan case study, on-glacier air temperatures at short flowline distances are more climate sensitive (i.e. demonstrate a relationship with off-glacier air temperature that is closer to 1). We therefore confirm earlier evidence regarding the high sensitivity of small glaciers (flowline distances < 1000 m) to external climate, and thus future warming.
2. The largest offsets between observed on-glacier and estimated off-glacier air temperatures are found for the warmest off-glacier hours, during drier, clear sky conditions of the summer monsoon period.
3. Above the established onset of the katabatic boundary layer, climatic sensitivity to ambient temperature decreases rapidly up to ~2000-3000 m along the glacier flowline. Beyond this distance, both the Tibetan glaciers and other datasets of the literature show a slower decrease of climatic sensitivity.
4. A parameterisation for the climatic sensitivity of the Tibetan study glaciers implies a smaller boundary layer effect than the existing parameterisation of Shea and Moore (2010). The climatology of a given region may influence the magnitude of the glacier's climatic sensitivity, though no clear relationships with the climatology of the glacier sites are found, thus suggesting the stronger role of local meteorological or topographic effects on the along-flowline pattern of T_a variability.
5. The terminus of some glaciers remain associated with other warm air processes, possibly due to boundary layer divergence, warm up-valley winds or debris cover heating. We find that these effects are evident only beyond ~70% of the total glacier flowline distance, although further work is required to explain this behaviour. A better understanding of temperature variability for this lower 30% is highly important as most of the summer melting will occur for this sector of the glacier.

In summarising the findings from all available distributed on-glacier datasets to date, we identify some key directions for future work on this subject. This includes comparing local influences of glacier size and micro-meteorology and standardising measurement practices, where possible, to aid the conclusions for a generalised model of on-glacier air temperature estimation.

Acknowledgements

Funding for the instrumentation of the Parlung catchment was provided by NSFC project (91647205 and 4191101270) and Newton Advanced Fellowship (NA170325). Á. Ayala acknowledges support from a FONDECYT project (number 3190732) and C. Bravo from the ANID Becas Chile PhD scholarship program. F. Pellicciotti acknowledges an ERC Consolidator Grant: 'RAVEN' (Rapid mass loss of debris covered glaciers in High Mountain Asia, grant agreement no. 772751). The authors kindly acknowledge the sharing of global datasets or parameters provided to aid this analysis, explicitly M. Nolan (McCall Glacier), J. Pomeroy, D. Pradhananga and the Global Water Futures Programme (Peyto Glacier), P. Smeets and IMAU, Utrecht (Pasterze Glacier), DGA, Chile (Universidad Glacier and Greve Glacier) and L. Carturan (AVDM, Italy). E. Ludewig is thanked for the provision of off-glacier temperature records at Sonnblick station, Austria. Additionally we recognise the hard work involved in obtaining and sharing all of the datasets acquired and the acknowledgements of those works.

Author contributions

TES and WY discussed and designed the research plan with Parlung data provided by WY and CZ. Additional data and analysis was provided by AA and CB. TES wrote the manuscript with scientific input from all co-authors.

Data availability

Calculated flowlines and climatic sensitivities are available at the following Zenodo repository: http://doi.org/10.5281/zenodo.3937777

Competing Interests

The authors declare that they have no conflicting interests.

References

ASF DAAC: ALOS PALSAR_Radiometric_Terrain_Corrected_low_res; Includes Material © JAXA/METI 2007. Accessed through ASF DAAC 20th March, 2020. DOI: 10.5067/JBYK3J6HFSVF, 2020

Arnold, N. S., Rees, W. G., Hodson, A. J., & Kohler, J.: Topographic controls on the surface energy balance of a high Arctic valley glacier. J. Geophys. Res, 111(F2), F02011. https://doi.org/10.1029/2005JF000426, 2006

Ayala, A., Pellicciotti, F., & Shea, J.: Modeling 2m air temperatures over mountain glaciers: Exploring the influence of katabatic cooling and external warming. J. Geophys. Res: Atmos, 120, 1–19. https://doi.org/10.1002/2015JD023137 , 2015

Betts, A. K., Chan, D. Z., & Desjardins, R. L.: Near-Surface Biases in ERA5 Over the Canadian Prairies. Front. Environ. Sci., 7. https://doi.org/10.3389/fenvs.2019.00129 , 2019

Bonekamp, P. N. J., Heerwaarden, C. C. Van, Steiner, J. F., & Immerzeel, W. W.: Using 3D turbulence-resolving simulations to understand the impact of surface properties on the energy balance of a debris-covered glacier. Cryosph, 14, 1611–1632. https://doi.org/10.5194/tc-14-1611-2020 , 2020

Bravo, C., Quincey, D. J., Ross, A. N., Rivera, A., Brock, B. W., Miles, E., & Silva, A.: Air Temperature Characteristics , Distribution , and Impact on Modeled Ablation for the South

Patagonia Ice field. J. Geophys. Res: Atmos, 124, 907–925. https://doi.org/10.1029/2018JD028857 , 2019

Bravo, C., Lorlaux, T., Rivera, A., & Brock, B. W.: Assessing glacier melt contribution to streamflow at Universidad Glacier, central Andes of Chile. Hydrol. Earth Syst. Sci, 21, 3249–3266. https://doi.org/10.5194/hess-21-3249-2017 , 2017

Brock, B. W., Mihalcea, C., Kirkbride, M. P., Diolaiuti, G., Cutler, M. E. J., & Smiraglia, C.: Meteorology and surface energy fluxes in the 2005–2007 ablation seasons at the Miage debris-covered glacier, Mont Blanc Massif, Italian Alps. J. Geophys. Res, 115, D09106. https://doi.org/10.1029/2009JD013224 , 2010

Caidong, C., & Sorteberg, A.: Modelled mass balance of Xibu glacier, Tibetan Plateau: Sensitivity to climate change. J. Glaciol, 56(196), 235–248. https://doi.org/10.3189/002214310791968467 , 2010

Carturan, L., Cazorzi, F., De Blasi, F., & Dalla Fontana, G.: Air temperature variability over three glaciers in the Ortles–Cevedale (Italian Alps): effects of glacier fragmentation, comparison of calculation methods, and impacts on mass balance modeling. Cryosph., 9(3), 1129–1146. https://doi.org/10.5194/tc-9-1129-2015 , 2015

Copernicus Climate Change Service (C3S): ERA5: Fifth generation of ECMWF atmospheric reanalyses of the global climate . Copernicus Climate Change Service Climate Data Store (CDS), Available at: https://cds.climate.copernicus.eu/cdsapp#!/home. Accessed 05/05/2020 , 2017

Ding, B., Yang, K., Yang, W., He, X., Chen, Y., Lazhu, … Yao, T.: Development of a Water and Enthalpy Budget-based Glacier mass balance Model (WEB-GM) and its preliminary validation. Water Resour. Res., 53(4), 3146–3178. https://doi.org/10.1002/2016WR018865 , 2017

Gabbi, J., Carenzo, M., Pellicciotti, F., Bauder, A., & Funk, M.: A comparison of empirical and physically based glacier surface melt models for long-term simulations of glacier response. J. Glaciol, 60(224), 1140–1154. https://doi.org/10.3189/2014JoG14J011 , 2014

Gardner, A. S., Sharp, M. J., Koerner, R. M., Labine, C., Boon, S., Marshall, S. J., … Lewis, D.: Near-Surface Temperature Lapse Rates over Arctic Glaciers and Their Implications for Temperature Downscaling. J. Clim., 22(16), 4281–4298. https://doi.org/10.1175/2009JCLI2845.1, 2009

Georges, C., & Kaser, G.: Ventilated and unventilated air temperature measurements for glacier-climate studies on a tropical high mountain site. J. Geophys. Res., 107(D24), 4775. https://doi.org/10.1029/2002JD002503 , 2002

Greuell, W., & Böhm, R.: 2 m temperatures along melting mid-latitude glaciers , and implications for the sensitivity of the mass balance to variations in temperature. J. Glaciol, 44(146), 9–20. , 1998

Greuell, W., Knap, W. H., & Smeets, P. C.: Elevational changes in meteorological variables along a midlatitude glacier during summer. J. Geophys. Res., 102(D22), 25941. https://doi.org/10.1029/97JD02083 , 1997

Hannah, D. M., Gurnell, A. M., & McGregor, G. R.: Spatio-temporal variation in microclimate, the surface energy balance and ablation over a cirque glacier. Int. J. Climatol., 20(7), 733–758. https://doi.org/10.1002/1097-0088(20000615)20:7 , 2000

https://doi.org/10.5194/tc-2020-198
Preprint. Discussion started: 12 August 2020

Heynen, M., Miles, E., Ragettli, S., Buri, P., Immerzeel, W., & Pellicciotti, F.: Air temperature variability in a high elevation Himalayan catchment. Ann. Glaciol., 57(71),. https://doi.org/10.3189/2016AoG71A076 , 2016

Huintjes, E., Sauter, T., Schröter, B., Maussion, F., Yang, W., Kropácek, J., … Schneider, C.: Evaluation of a Coupled Snow and Energy Balance Model for Zhadang Glacier, Tibetan Plateau, Using Glaciological Measurements and Time-Lapse Photography. Arctic, Antarct. Alp. Res., 47(3), 573–590. https://doi.org/10.1657/AAAR0014-073 , 2015

Immerzeel, W. W., Petersen, L., Ragettli, S., & Pellicciotti, F.: The importance of observed gradients of air temperature and precipitation for modeling runoff from a glacierized watershed. Water Resour. Res., 50, 2212–2226. https://doi.org/10.1002/2013WR014506. , 2014

Jiskoot, H., & Mueller, M. S.: Glacier fragmentation effects on surface energy balance and runoff: field measurements and distributed modelling. Hydrol. Process., 26(12), 1861–1875. https://doi.org/10.1002/hyp.9288 , 2012

Jobst, A. M., Kingston, D. G., Cullen, N. J., & Sirguey, P.: Combining thin-plate spline interpolation with a lapse rate model to produce daily air temperature estimates in a data-sparse alpine catchment. Int. J. Climatol.. https://doi.org/10.1002/joc.4699 , 2016

Marshall, S. J., Sharp, M. J., Burgess, D. O., & Anslow, F. S.: Near-surface-temperature lapse rates on the Prince of Wales Icefield, Ellesmere Island, Canada: implications for regional downscaling of temperature. Int. J. Climatol., 27, 1549-1555. https://doi.org/10.1002/joc , 2007

Maurer, J. M., Schaefer, J. M., Rupper, S., & Corley, A.: Acceleration of ice loss across the Himalayas over the past 40 years. Sci. Adv., 5, 1–12., 2019

Minder, J. R., Mote, P. W., & Lundquist, J. D.: Surface temperature lapse rates over complex terrain: Lessons from the Cascade Mountains. J. Geophys. Res., 115(D14), D14122. https://doi.org/10.1029/2009JD013493 , 2010

Mölg, T., Maussion, F., Yang, W., & Scherer, D.: The footprint of Asian monsoon dynamics in the mass and energy balance of a Tibetan glacier. Cryosph., 6(6), 1445–1461. https://doi.org/10.5194/tc-6-1445-2012 , 2012

Munro, D. S.: Linking the weather to glacier hydrology and mass balance at Peyto glacier. Peyto Glacier: One Century of Science. National Hydrology Research Institute Science Report #8. , 2006

Munro, D. S., & Marosz-Wantuch, M.: Modeling Ablation on Place Glacier, British Columbia, from Glacier and Off-glacier Data Sets. Arctic, Antarct. Alp. Res., 41(2), 246–256. https://doi.org/10.1657/1938-4246-41.2.246 , 2009

Nolin, A. W., Phillippe, J., Jefferson, A., & Lewis, S. L.: Present-day and future contributions of glacier runoff to summertime flows in a Pacific Northwest watershed: Implications for water resources. Water Resour. Res., 46(12). https://doi.org/10.1029/2009WR008968 , 2010

Oerlemans, B. J., & Grisogono, B.: Glacier winds and parameterisation of the related surface heat fluxes. Tellus, 54, 440–452. , 2002

Oerlemans, J.: The microclimate of valley glaciers. Utrecht Publishing and Archiving Services, Universiteitsbibliotheek, Utrecht. , 2010

https://doi.org/10.5194/tc-2020-198
Preprint. Discussion started: 12 August 2020

Oerlemans, J.: Glaciers and Climate Change. , 2001

Pellicciotti, F., Helbing, J., Rivera, A., Favier, V., Corripio, J. G., Araos, J., … Carenzo, M.: A study of the energy balance and melt regime on Juncal Norte Glacier , semi-arid Andes of central Chile , using melt models of different complexity. Hydrol. Process., 22, 3980–3997. https://doi.org/10.1002/hyp , 2008

Petersen, L., & Pellicciotti, F.: Spatial and temporal variability of air temperature on a melting glacier: Atmospheric controls, extrapolation methods and their effect on melt modeling, Juncal Norte Glacier, Chile. J. Geophys. Res., 116(D23), D23109. https://doi.org/10.1029/2011JD015842 , 2011

Petersen, L., Pellicciotti, F., Juszak, I., Carenzo, M., & Brock, B. W.: Suitability of a constant air temperature lapse rate over an Alpine glacier: testing the Greuell and Böhm model as an alternative. Ann. Glaciol., 54(63), 120–130. https://doi.org/10.3189/2013AoG63A477 , 2013

Ragettli, S., Immerzeel, W. W., & Pellicciotti, F.: Contrasting climate change impact on river flows from high-altitude catchments in the Himalayan and Andes Mountains. Proc. Natl. Acad. Sci., 113(33). https://doi.org/10.1073/pnas.1606526113 , 2016

Rets, E. P., Popovnin, V. V, Toropov, P. A., Smirnov, A. M., Tokarev, I. V, Chizhova, J. N., … Kireeva, M. B.: Djankuat glacier station in the North Caucasus , Russia : a database of glaciological , hydrological , and meteorological observations and stable isotope sampling results during 2007 – 2017. Earth Syst. Sci. Data, 1463–1481. https://doi.org/https://doi.org/10.5194/essd-11-1463-2019 , 2019

Sauter, T., & Galos, S. P.: Effects of local advection on the spatial sensible heat flux variation on a mountain glacier. Cryosph., 10, 2887–2905. https://doi.org/10.5194/tc-10-2887-2016 , 2016

Schwanghart, W., Kuhn, N, J.: TopoToolbox: A set of Matlab functions for topographic analysis, Environmental Modelling & Software, 25 (6), 770-781. https://doi.org/10.1016/j.envsoft.2009.12.002. , 2010

Shaw, T. E., Brock, B. W., Ayala, A., Rutter, N., & Pellicciotti, F.: Centreline and cross-glacier air temperature variability on an Alpine glacier: assessing temperature distribution methods and their influence on melt model calculations. J. Glaciol, 1–16. https://doi.org/10.1017/jog.2017.65 , 2017

Shaw, T., Brock, B., Fyffe, C., Pellicciotti, F., Rutter, N., & Diotri, F.: Air temperature distribution and energy balance modelling of a debris-covered glacier. J. Glaciol, 62(231), 185–198. https://doi.org/10.1017//jog.2016.31 , 2016

Shea, J. M., & Moore, R. D.: Prediction of spatially distributed regional-scale fields of air temperature and vapor pressure over mountain glaciers. J. Geophys. Res., 115(D23), D23107. https://doi.org/10.1029/2010JD014351 , 2010

Steiner, J. F. and Pellicciotti, F.: Variability of air temperature over a debris-covered glacier in the Nepalese Himalaya, Ann. Glaciol., 57(71), 295–307, doi:10.3189/2016AoG71A066, 2016.

Strasser, U., Corripio, J. G., Pellicciotti, F., Burlando, P., Brock, B. W., & Funk, M.: Spatial and temporal variability of meteorological variables at Haut Glacier d'Arolla (Switzerland) during the ablation season 2001: Measurements and simulations. J. Geophys. Res., 109, D03103. https://doi.org/10.1029/2003JD003973 , 2004

Troxler, P., Ayala, Á., Shaw, T. E., Nolan, M., Brock, B. W., & Pellicciotti, F.: Modelling spatial patterns of near-surface air temperature over a decade of melt seasons on McCall Glacier, Alaska. J. Glaciol, 1–15. https://doi.org/https://doi.org/10.1017/jog.2020.12 , 2020

van de Wal, R. S. W., Oerlemans, J., & Van Der Hage, J. C.: A study of ablation variations on the tongue of Hintereisferner, Austrian Alps. J. Glaciol, 38(130), 319–324. , 1992

van den Broeke, M. R.: Momentum , Heat , and Moisture Budgets of the Katabatic Wind Layer over a Midlatitude Glacier in Summer. J. Appl. Meteorol., 36(1987), 763–774. , 1997

Wang, R., Liu, S., Shangguan, D., Radić, V., & Y, Z.: Spatial Heterogeneity in Glacier Mass-Balance. Water, 11(776), 1–21. https://doi.org/doi:10.3390/w11040776 , 2019

Yang, W., Guo, X., Yao, T., Yang, K., Zhao, L., Li, S., & Zhu, M.: Summertime surface energy budget and ablation modeling in the ablation zone of a maritime Tibetan glacier. J. Geophys. Res. Atmos, 116(14), 1–11. https://doi.org/10.1029/2010JD015183 , 2011

Yang, W., Yao, T., Guo, X., Zhu, M., Li, S., & Kattel, D. B.: Mass balance of a maritime glacier on the southeast Tibetan Plateau and its climatic sensitivity. J. Geophys. Res. Atmos, 118(17), 9579–9594. https://doi.org/10.1002/jgrd.50760 , 2013

Zhao, L., Tian, L., Zwinger, T., Ding, R., Zong, J., Ye, Q., & Moore, J. C.: Numerical simulations of Gurenhekou glacier on the Tibetan Plateau. J. Glaciol, 60(219), 71–82. https://doi.org/10.3189/2014JoG13J126 , 2014

Zhu, M., Yao, T., Yang, W., Maussion, F., Huintjes, E., & Li, S.: Energy- and mass-balance comparison between Zhadang and Parlung No. 4 glaciers on the Tibetan Plateau. J. Glaciol, 61(227), 595–607. https://doi.org/10.3189/2015JoG14J206 , 2015

Figures

https://doi.org/10.5194/tc-2020-198
Preprint. Discussion started: 12 August 2020

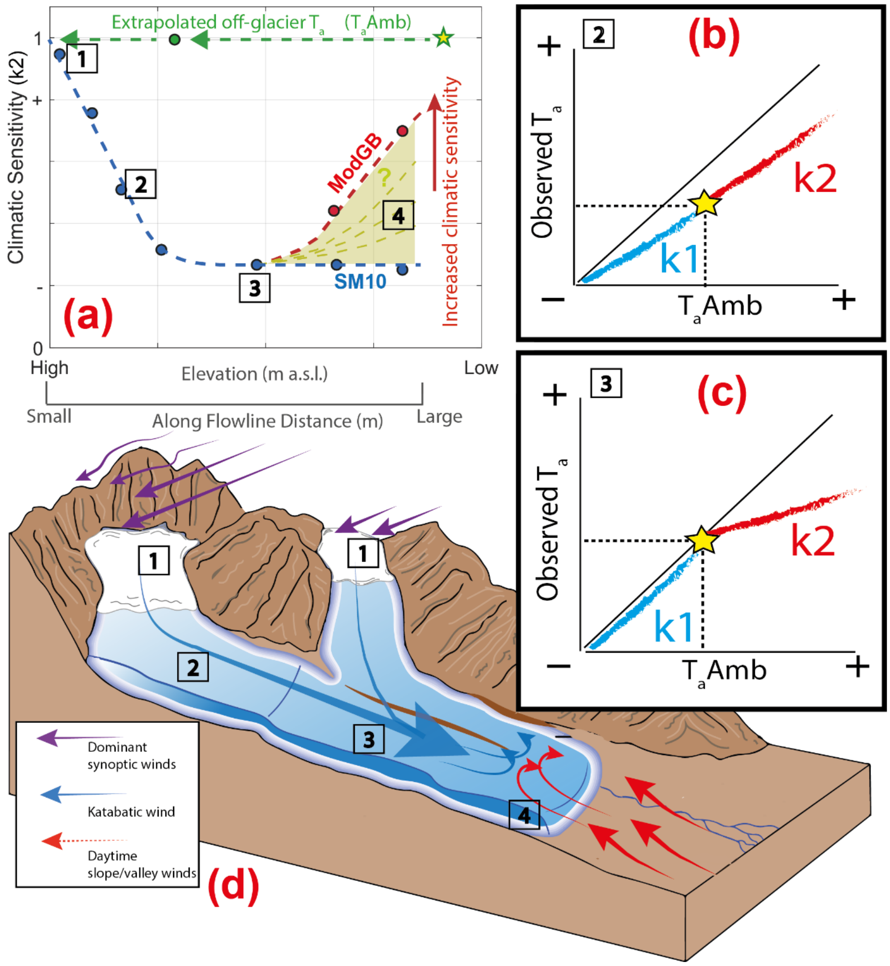

Figure 1: A schematic diagram to describe the climatic sensitivity of on-glacier air temperature (T_a) to the extrapolated ambient temperature ($T_a$amb) at given elevations/flowline distances on a mountain glacier. Points 1-4 indicate locations of interest in the context of the current science for this topic that are linked between panels. Panel (a) indicates the along-flowline 'k2' climatic sensitivities to T_aAmb, considering down-glacier decrease in sensitivities and the observed differences in the models of SM10 and ModGB for glacier termini (see text). While ModGB does not explicitly include the k2 parameter, its approach is similar to considering an increasing climatic sensitivity to T_aAmb (see Ayala et al., 2015). The green line in panel (a) indicates the local off-glacier lapse rate to estimate T_aAmb using off-glacier observations at varying elevations (green dot). Panels (b) and (c) represent the differences of k1 and k2 sensitivities observed in the data at different theoretical locations on the glacier (see Figure 5, for examples on Parlung glaciers), the latter of which shows the theoretical parameterisation presented by Shea and Moore (2010). Panel (d) represents an idealised case of katabatic and valley/synoptic wind interactions that potentially dictate the along-flowline structure of on-glacier climatic sensitivity and thus T_a estimation.

https://doi.org/10.5194/tc-2020-198
Preprint. Discussion started: 12 August 2020

The Cryosphere
Discussions
Open Access
EGU

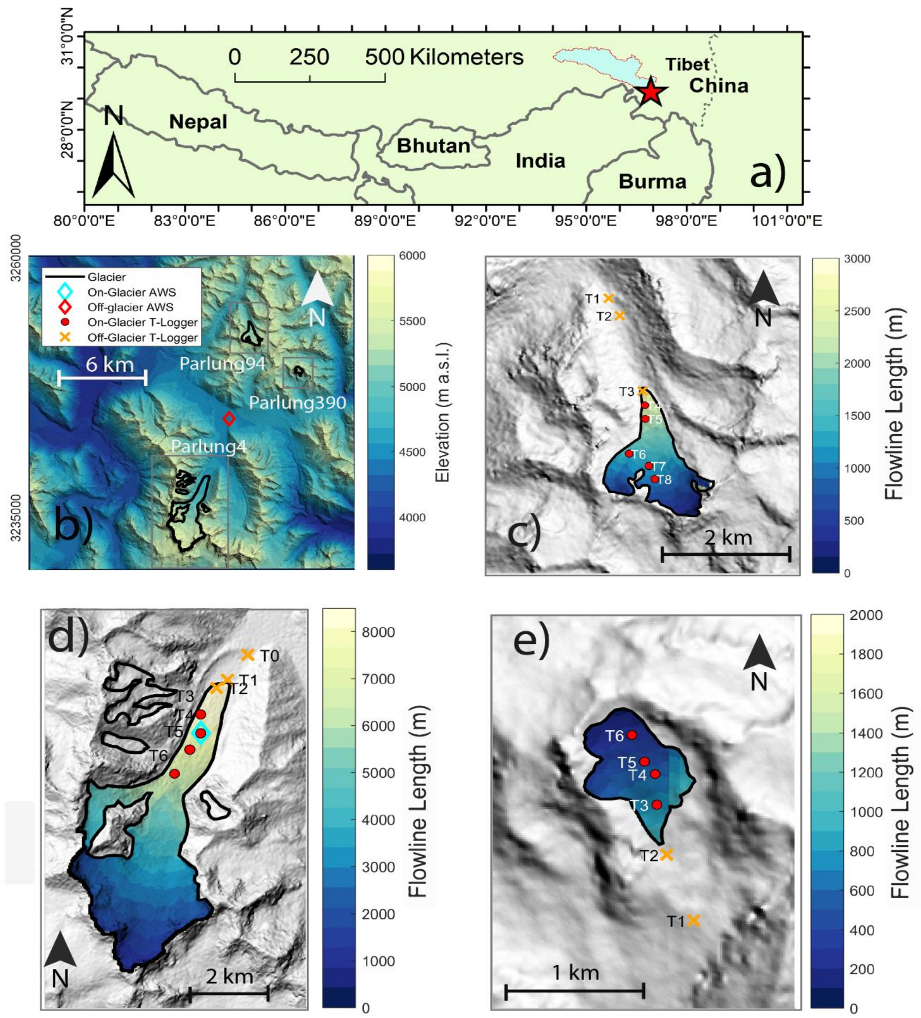

Figure 2: The location of Parlung catchment in Tibet (a) and a map of the Parlung catchment (b) with the study glaciers, Parlung 94 (c), Parlung4 (d) and Parlung390 (e). Off-glacier and on-glacier AWS and T-Logger locations are shown (without glacier number suffix). (a) shows the elevation of the catchment (DEM source: Alos Palsar) and (b-d) show the calculated flowline distances based upon TopoToolbox (scales vary).

https://doi.org/10.5194/tc-2020-198
Preprint. Discussion started: 12 August 2020

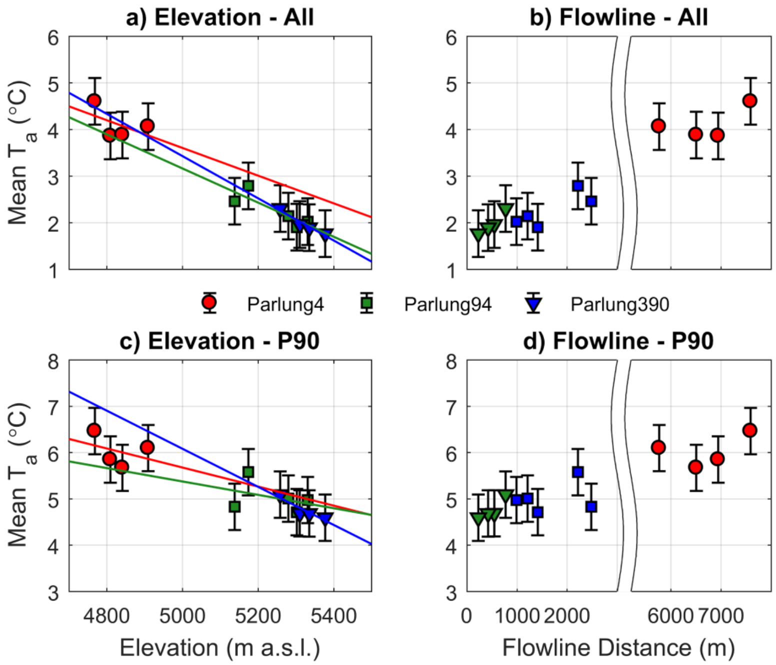

867
868 *Figure 3: The elevation-mean T_a and uncertainty (errorbar) for (a) all hours and (c) P90 hours (n = 312).*
869 *Panels (b) and (d) are the equivalent plots against flowline distance. Coloured lines show the linear fit*
870 *against elevation ('lapse rate') to each glacier. An x-axis scale break is used in (b) and (d) for clarity.*
871
872

https://doi.org/10.5194/tc-2020-198
Preprint. Discussion started: 12 August 2020

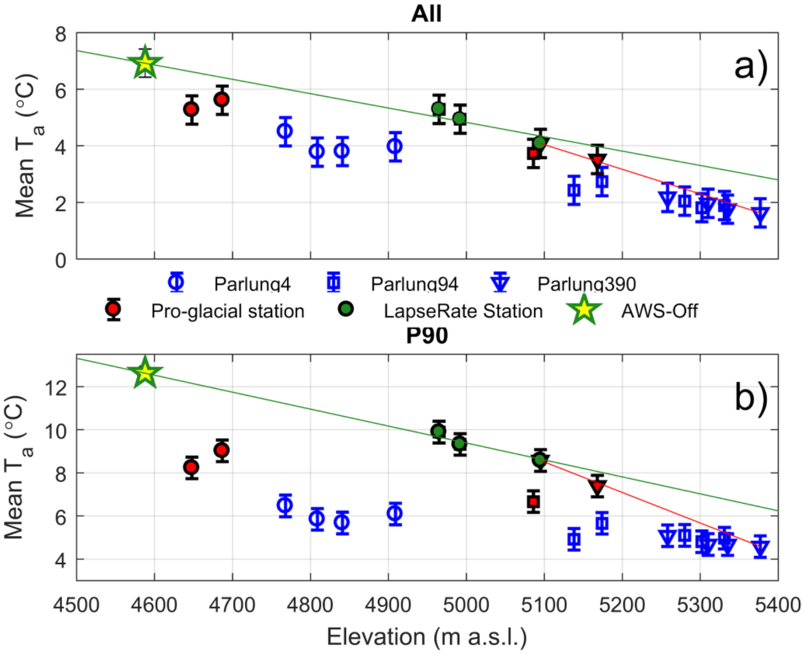

Figure 4: The mean T_a against elevation for all hours (a) and P90 hours (b), where blue markers are on-glacier T-Loggers, red markers are pro-glacial T-Loggers and green circles denote off-glacier T-Loggers used to construct an hourly variable 'catchment lapse rate' (green line), extrapolated from AWS_Off (star). The red line indicates the piecewise lapse rate above the elevation of T1_390 to lapse T_a to the top of the flowline. A 0.5°C uncertainty is shown by the errorbar for each station (not applied to the lapse rate for neatness).

https://doi.org/10.5194/tc-2020-198
Preprint. Discussion started: 12 August 2020

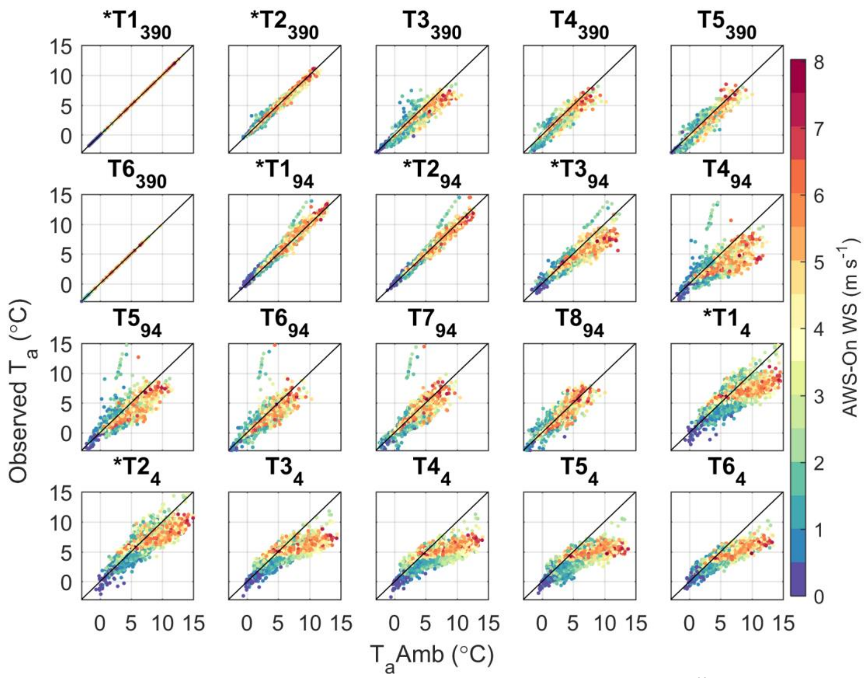

*Figure 5: Estimated (T_aAmb) vs Observed T_a at each T-Logger location (including off-glacier T-Loggers). Individual, hourly values are coloured by the observed wind speeds at AWS_On (Parlung4). No on-glacier wind speed data exist for Parlung94 and Parlung390, so the coloured markers are only assumed for those glaciers from the parlung4 wind speed data. * denotes stations that are off-glacier.*

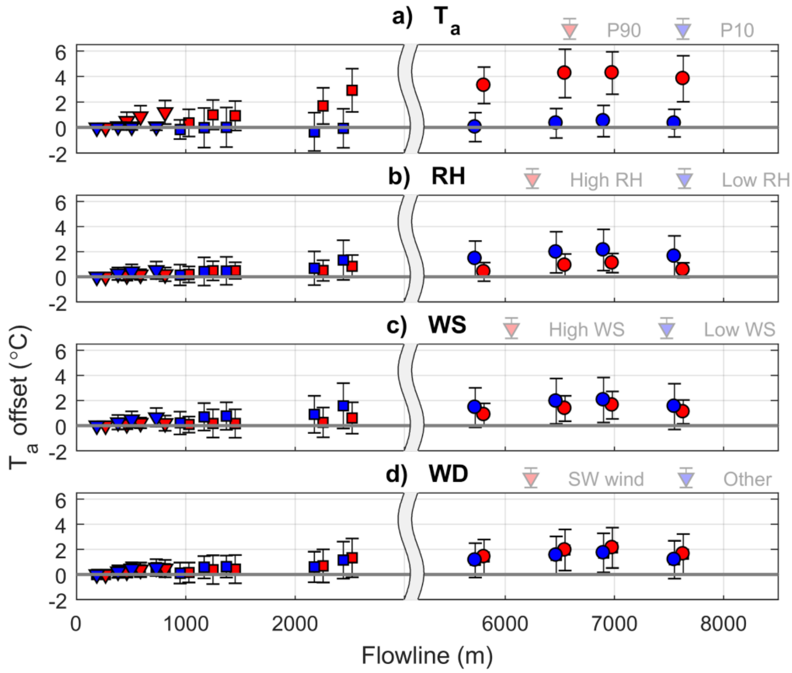

Figure 6: The mean and standard deviation (error-bars) of hourly T_a bias offsets (estimated-observed) along the glacier flowline. Each panel depicts hourly grouping by (a) off-glacier T_a at AWS_Off (P90 is ≥ 10.5 °C and P10 is ≤ 3.5 °C), (b) off-glacier RH at AWS_Off (high is > 90 % and low is < 70 %), (c) wind speed from ERA5 (high = > 2.5 m s^{-1} and low = < 0.7 m s^{-1}) and (d) dominant wind direction from ERA5 (Southwest wind direction is considered as 180-270°). Marker shapes show the different glaciers, as in Figure 3 and 4.

https://doi.org/10.5194/tc-2020-198
Preprint. Discussion started: 12 August 2020

The Cryosphere
Discussions
Open Access

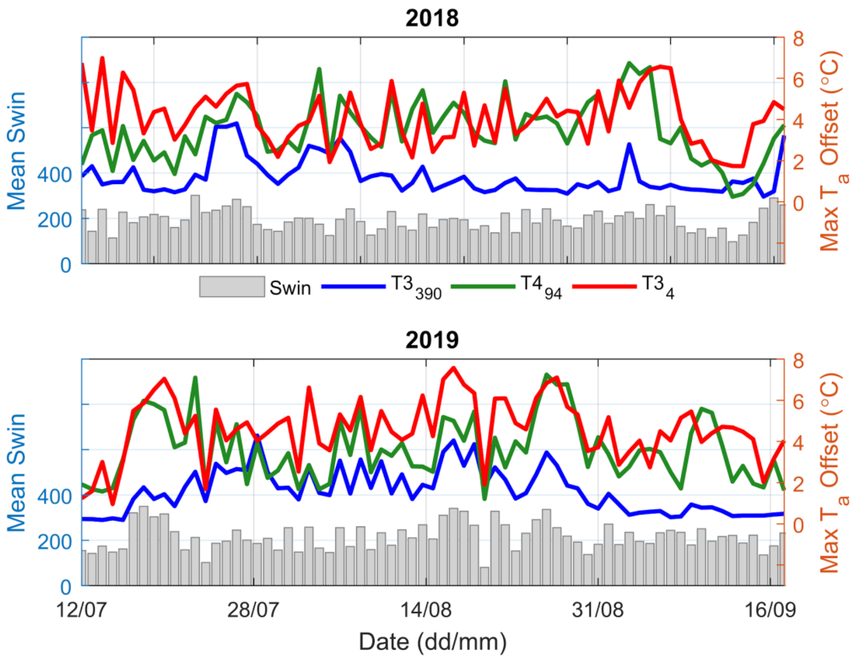

899

900 *Figure 7: Maximum daily T_a offsets (estimated - observed) at the most distant along-flowline T-Loggers on*
901 *each glacier for (top) and 2019 (bottom). Mean daily incoming shortwave radiation at AWS_Off is shown*
902 *by the grey bars.*

903

https://doi.org/10.5194/tc-2020-198
Preprint. Discussion started: 12 August 2020

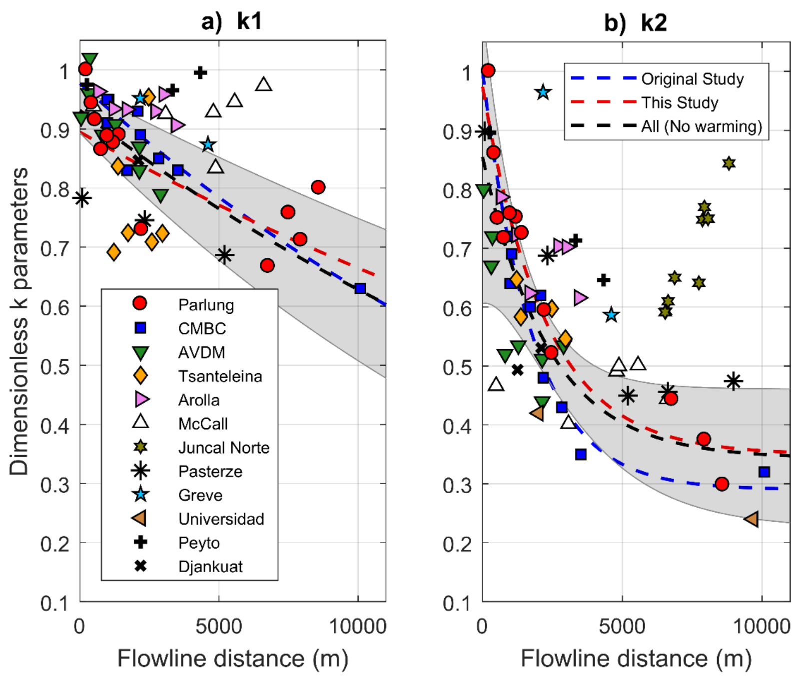

904
905 *Figure 8: The calculated k1 and k2 sensitivities as a function of the flowline distance of each observation*
906 *on the Parlung glaciers (red circles) and other, global datasets (Table 2). The dashed blue and red lines*
907 *show the fitted exponential parameterisation of Shea and Moore (2010) and this study, respectively. The*
908 *dashed black line and shaded area denotes the equivalent parameterisation for all observations where a*
909 *large increase in sensitivity on the glacier terminus ('warming effect') is absent (explicitly excluding data*
910 *from McCall, Juncal Norte and Djankuat). The shaded area represents the 95% confidence interval of this*
911 *fit line.*

https://doi.org/10.5194/tc-2020-198
Preprint. Discussion started: 12 August 2020

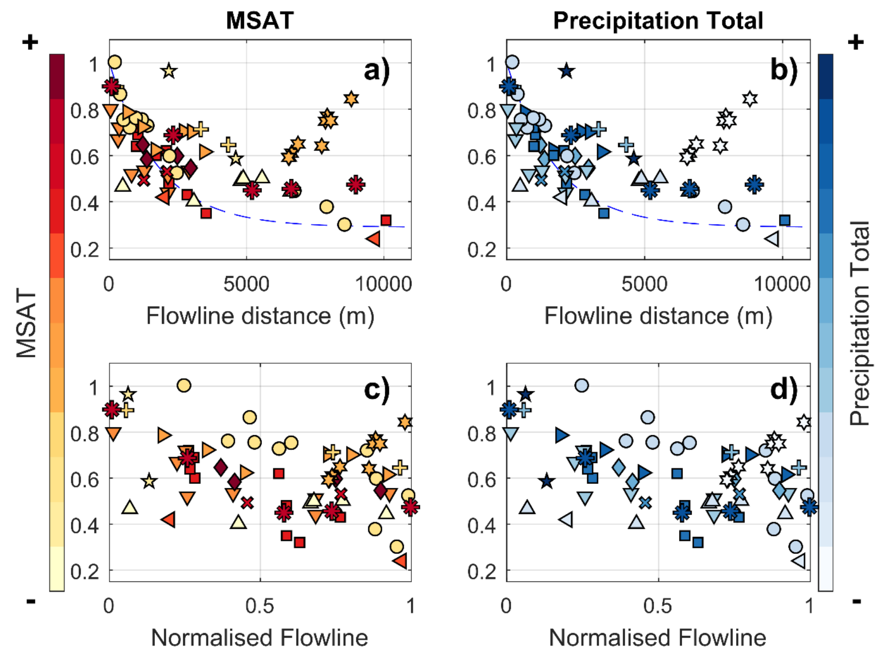

Figure 9: The k2 sensitivities as a function of flowline distance (top) and a normalized distance, considering the total flowline distance for the year of study (bottom). The individual glaciers of grouped studies (Parlung, CMBC and AVDM) are separated and normalized by the individual glacier length (symbols as in Figure 8). Glaciers are coloured by rankings of the mean summer air temperatures (MSAT - left) and precipitation total (PT - right). The original parameterisation is retained in the top panels.

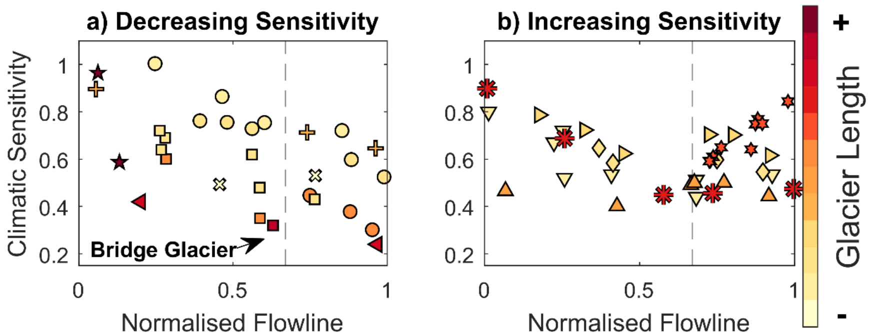

Figure 10: The k2 sensitivity along the normalized flowline compared to total glacier length (colour bar) and subjectively grouped by the evidence of a relative warming effect (increasing climatic sensitivity) toward the glacier terminus.

https://doi.org/10.5194/tc-2020-198
Preprint. Discussion started: 12 August 2020

Tables

Table 1: Details of each AWS/T-Logger station used in this analysis including the calculated flowline distances.

Station	Latitude	Longtitude	Elevation (m a.s.l.)	Flowline (m)	on/off glacier
AWS_Off	29.314	96.955	4588	-	off
AWS_On	29.500	97.009	4649	-	off
$T1_{390}$	29.348	97.022	5095	-	off
$T2_{390}$	29.352	97.020	5168	-	off
$T3_{390}$	29.354	97.0202	5258	770	on
$T4_{390}$	29.356	97.020	5310	544	on
$T5_{390}$	29.357	97.019	5335	420	on
$T6_{390}$	29.359	97.018	5377	224	on
$T1_{94}$	29.621	97.218	4965	-	off
$T2_{94}$	29.417	96.99	4992	-	off
$T3_{94}$	29.635	96.975	5086	-	off
$T4_{94}$	29.596	97.065	5138	2481	on
$T5_{94}$	29.56	97.067	5174	2215	on
$T6_{94}$	29.466	97.023	5302	1411	on
$T7_{94}$	29.434	97.080	5280	1208	on
$T8_{94}$	29.399	97.097	5331	988	on
$T1_{4}$	29.271	96.968	4690	-	off
$T2_{4}$	29.368	96.935	4769	-	off
$T3_{4}$	29.298	97.168	4809	8589	on
$T4_{4}$	29.298	97.168	4809	7940	on
$T5_{4}$	29.496	97.126	4841	7505	on
$T6_{4}$	29.403	97.068	4909	6765	on

https://doi.org/10.5194/tc-2020-198
Preprint. Discussion started: 12 August 2020

Table 2: The details of each site where distributed on-glacier air temperatures are available. Elevation ranges and mean summer air temperatures (MSAT) are reported for the year of investigation. Precipitation totals (mm – 'PT') was obtained upon cited literature.

Site	Lat	Lon	Year(s)	Elevation	MSAT	PT	T_a Data Reference
				m .a.s.l.	°C	mm	
Parlung (Tibet)	29.24	96.93	2018-2019	4600-5800	2.19	679	This Study
CMBC (Canada)	50.32	-122.48	2006-2008	1375-2898	10.29	1113	Shea and Moore (2010)
AVDM (Italy)	46.42	10.62	2010-2011	2650-3769	7.94	784	Carturan et al. (2015)
Tsanteleina (Italy)	45.48	7.06	2015	2800-3445	13.76	805	Shaw et al., (2017)
Arolla (Switzerland)	45.97	7.52	2010	2550-3520	7.28	1663	Ayala et al. (2015)
McCall (USA)	69.31	-143.85	2004-2014	1375-2365	-2.28	500	Troxler et al. (2020)
Juncal Norte (Chile)	-33.01	-70.09	2007-2008	2900-5910	6.58	352	Ayala et al. (2015)
Greve (Chile)	-48.88	-73.52	2015-2016	0-2400	-0.1	12000	Bravo et al. (2019)
Pasterze (Austria)	47.09	12.71	1994	2150-3465	12.66	2761	Greuell and Böhm, (1998)
Universidad (Chile)	-34.69	-70.33	2009-2010	2463-4543	8.24	474	Bravo et al. (2017)
Peyto (Canada)	51.66	-116.55	2011	2260-3000	2.94	800	Pradhananga et al. (2020)*
Djankuat (Russia)	43.20	42.77	2017	3210-4000	12.13	950	Rets et al. (2019)

**paper not yet submitted*

Table 3: The coefficients of the original SM10 model and those fit to the k1 and k2 sensitivities on the Parlung glaciers and all glaciers where no warming effect was evident (see Figure 10).

Model	k1 = β1*exp(β2*DF)	k2 = β3 + β4*exp(-β5*DF)
CMBC (Shea and Moore, 2010)	*β1* = **0.977** *β2* = **-4.4e-5**	*β3* = **0.29** *β4* = **0.71** *β5* = **5.6e-4**
Parlung	*β1* = **0.894** (0.805,0.983) *β2* = **-2.972e-5** (-5.543e-5,-4.0e-6)	*β3* = **0.349** (0.241,0.456) *β4* = **0.624** (0.492,0.757) *β5* = **4.4e-3** (1.7e-4,7.2e-4)
All (no increased sensitivity on glacier terminus)	*β1* = **0.923** (0.886,0.96) *β2* = **-3.375e-5** (-5.543e-5,-4.0e-6)	*β3* = **0.343** (0.225,0.46) *β4* = **0.511** (0.38,0.642) *β5* = **4.2e-3** (1.5e-4,6.9e-4)